Single-fluorophore imaging with an unmodified epifluorescence microscope and conventional video camera

K. ADACHI,*‡ K. KINOSITA, JR†‡ & T. ANDO*

Department of Physics, Faculty of Science, Kanazawa University, Kakuma-machi, Kanazawa 920-1192, Japan

†*Department of Physics, Faculty of Science and Technology, Keio University, Kohoku-Ku, Yokohama 223-8522, Japan*

‡*CREST (Core Research for Evolutional Science and Technology) 'Genetic Programming' Team 13, Nogawa, Miyamae-ku, Kawasaki 216-0001, Japan*

Summary

Single fluorophores in aqueous solution were imaged in real time with a conventional silicon-intensified target video camera connected to an unmodified commercial microscope (IX70, Olympus) with epifluorescence excitation with a high-pressure mercury lamp. Neither a powerful laser nor an extremely sensitive video camera was required. Three experimental systems were used to demonstrate quantitatively that individual, moving or stationary Cy3 fluorophores could be imaged with the microscope: Cy3-gelsolin attached to an actin filament sliding over heavy meromyosin, sliding actin filaments sparsely labelled with Cy3, and heavy meromyosin labelled with one or two Cy3 fluorophores. The results should encourage many laboratories to attempt 'single-molecule physiology' in which the functions and mechanisms of molecular machines are studied at the single-molecule level in an environment where the biological machines are fully active.

Introduction

Single-fluorophore imaging (Moerner & Kador, 1989; Betzig & Chichester, 1993) is now becoming a versatile tool in many fields of science (Harada *et al.*, 1998). Studies at the level of single molecules have shown that identical molecules may exhibit 'individualism', in that individual behaviours are quite different from the ensemble average (Nishizaka *et al.*, 1995; de Gennes, 1997; Dickson *et al.*, 1997; Lu & Xie, 1997; Perkins *et al.*, 1997). The understanding of true molecular dynamics thus requires one-by-one examination of individual molecules. Single-fluorophore imaging is particularly suited for this purpose, because

Correspondence to: T. Ando. Tel: 076-264-5663; fax: 076-264-5739; e-mail: tando@kenroku.ipc.kanazawa-u.ac.jp

many molecules can be observed separately yet at the same time. Single-fluorophore imaging is also a key to the evolving field of 'single-molecule physiology' in which the mechanisms of molecular machines made of protein molecules are studied in an environment where the protein machines are fully functional. The stochastic nature of the operation of protein machines, in addition to the probable individualism, calls for single-molecule observations. Real-time imaging of single fluorophores in aqueous environments, where protein machines work, is now feasible; applications to date include the observations of chemical reaction in a single enzyme molecule (Funatsu *et al.*, 1995), translational (Sase *et al.*, 1995; Vale *et al.*, 1996) and rotational (Sase *et al.*, 1997) motions of molecular motors, and coupling between chemical and mechanical events in a molecular motor (Ishijima *et al.*, 1998). Real-time detection of conformational changes in individual protein machines should now be possible under an optical microscope (Kinosita *et al.*, 1997).

So far, single-fluorophore imaging has been somewhat demanding. The major requisite for single-fluorophore imaging, particularly important in aqueous environments where fluorescence tends to be weak, is the reduction of background luminescence, which may originate in any optical elements and in the sample itself. Confining the excitation light is one solution, and prism- (Funatsu *et al.*, 1995) or objective-type (Tokunaga *et al.*, 1997) total internal reflection microscopy has proved to be quite effective. However, restricted, and thus inhomogeneous, illumination limits its applicability, and the optical setup for evanescent excitation demands some skill. The most versatile and user-friendly method will be the use of a conventional epifluorescence microscope, but, so far, careful modifications including replacement of optical elements have been required to convert a commercial microscope

into a single-fluorophore imager (Funatsu *et al.*, 1995; Sase *et al.*, 1995). Also, all single-fluorophore imaging reported to date employs laser excitation, which, in combination with a highly sensitive video camera such as one equipped with an image intensifier, warrants bright images of individual fluorophores. However, lasers and sensitive cameras are expensive. An inexpensive system that does not require expert skill is desirable. Here we present evidence that single fluorophores in an aqueous solution can be imaged in real time in a conventional system consisting of an unmodified commercial microscope with a mercury lamp as the excitation source and a silicone-intensified target (SIT) camera. This should encourage researchers who are not in a microscopy-specialized laboratory to build their own single-molecule imager and to explore the behaviours of individual molecules.

Materials and methods

Video microscopy

A commercial epifluorescence microscope (IX70; Olympus, Japan) was used without modification. The excitation light source was a standard high-pressure mercury lamp (USH-102D; Ushio, Japan). A SIT video camera (C2741-08; Hamamatsu Photonics, Japan) was directly connected to the side video port of the microscope. In addition to a standard filter set (U-MWIG; Olympus, Japan) for epifluorescence observation, an emission bandpass filter (transmission at 562–618 nm; Chroma Technology, U.S.A.) was inserted before the video camera. An oil-immersion objective lens (PlanApo 60×, NA 1·4; Olympus, Japan) was used with an immersion oil supplied from Olympus ($n_d = 1·516$ at 23 °C). Coverslips (Micro Cover Glass, No.1, 18×18 mm^2 and 24×36 mm^2; Matsunami, Japan) were cleaned with 20 N KOH. Images were recorded on a Hi8 video recorder (EVO-9650; Sony, Japan) and analysed with a digital image processor (C2000; Hamamatsu Photonics, Japan).

Quantitative estimations of light intensity and light collection efficiency

The digital image processor together with the SIT video camera linearly converts the intensity of light arrived at each pixel into a numerical value (N_{AD}). To give a quantitative measure to N_{AD}, we carried out following measurements. The SIT video camera and the objective lens were replaced with a light-power meter (TQ1280, Advantest, Japan) and with an objective lens (UPlanFl, ×10, NA 0·3; Olympus, Japan), respectively. In the transillumination mode, diaphragmed light from a tungsten lamp, which was passed through a heat-absorbing filter (MBN11500; Nikon, Japan), was collected by the objective lens, and the power of

light collected, E_p, was measured. After the measurement the power meter was replaced with the video camera where neutral-density filters (total $9·3 \times 10^{-6}$% transmittance) were additionally inserted before the video camera. The diaphragmed light images were recorded and the image integrated over 16 video frames was digitized. The values of N_{AD} at all pixels within the diaphragmed light image were summed (I_p). Thus, the number of photons s^{-1} (N_p) corresponding to N_{AD} (in the single frame recording) is given by

$$N_p = \alpha \times N_{AD} \left(\alpha \equiv \frac{E_p}{hc} \lambda \frac{16 \times 9·3 \times 10^{-8}}{I_p} \right) \qquad (1)$$

where h, c and λ are Planck's constant, the speed of light and the wavelength of light (≈ 590 nm), respectively.

The number of photons emitted per second from a Cy3-actin protomer was calculated from various quantities such as the power of excitation light appearing after an objective lens (PlanApo 60×, NA 1·4; Olympus, Japan), the spectral irradiance of the high-pressure mercury lamp, the illumination area, the absorption spectrum of Cy3-actin and the quantum yield of Cy3-actin. The power of excitation light was measured by placing the light-power meter just above the objective lens. The efficiency of emission light collection was then estimated from the number of photons per second calculated above and the corresponding observed intensity expressed in the number of photons per second.

Proteins

Actin was extracted from acetone powder of rabbit skeletal muscles and purified by the method of Spudich & Watt (1971). Heavy meromyosin (HMM) was obtained by chymotryptically digesting rabbit skeletal myosin according to Weeds & Pope (1977). The molar concentration of F-actin was estimated from the extinction coefficient $E^{1\%}_{290nm} = 6·7$ (Ando, 1984) and a molecular weight of $4·2 \times 10^4$, after correction for turbidity (1·68 times the apparent absorbance at 330 nm was subtracted from the absorbance at 290 nm). The molar concentration of HMM was estimated from $E^{1\%}_{280nm} = 7·0$ (Ando & Scales, 1985) and a molecular weight of $3·5 \times 10^5$ (1·93 times the absorbance at 330 nm was subtracted from the absorbance at 280 nm). Gelsolin was prepared from bovine serum according to the method of Kurokawa *et al.* (1990). The molar concentration of gelsolin was estimated from $E^{1\%}_{280nm} = 15·4$ (Craig & Megerman, 1977), with the correction for turbidity, and a molecular weight of $8·6 \times 10^4$. Transglutaminase from *Streptoverticillium* was a gift from Ajinomoto Foods Co. (Japan); the enzyme was purified by DEAE ionic exchange HPLC (DEAE-5PW; Tosoh, Japan) as in Connellan *et al.* (1971).

Actin filaments with Cy3-labelled gelsolin at the tail end

Gelsolin, which binds to the barbed end of an actin filament (Suzuki *et al.*, 1996), was labelled with Cy3 by transglutaminase catalysis (Kunioka & Ando, 1996). First, Cy3-cadaverine was prepared by mixing 500 nmole dry, monofunctional Cy3-NHS-ester (Amersham Life Science, U.S.A.) with 50 μmole cadaverine in 0·5 mL of dry DMSO, followed by incubation for 24 h at 30 °C. The product was purified by reverse-phase HPLC (CN-80TS; Tosoh, Japan). Transglutaminase (0·5 units mL^{-1}) was incubated in a solution containing 4 mM dithiothreitol plus buffer A (50 mM TES, 1 mM EGTA, 0·3 M KCl, pH 7·0) at 4 °C overnight. Gelsolin (10 μM) was allowed to react with Cy3-cadaverine (1 mM) in the presence of transglutaminase (0·025 units mL^{-1}) in buffer A containing 2 mM dithiothreitol for 3·8 h at 25 °C. The reaction was terminated by cooling in ice-cold water. After centrifugation at 148 000 g for 10 min, gelsolin and transglutaminase in the supernatant were separated by gel filtration HPLC (G2000sw; Tosoh, Japan). The protein concentration in the labelled gelsolin fraction was determined by the method of Lowry *et al.* (1951), with a standard curve obtained for unlabelled gelsolin. The Cy3-labelled gelsolin (10 nM) was incubated with F-actin (5 μM) in a solution containing 25 mM KCl, 4 mM MgCl$_2$, 0·2 mM CaCl$_2$ and 25 mM imidazole-HCl (pH 7·6) for 30 min at room temperature. To stabilize the actin filaments, phalloidin (Molecular Probes, U.S.A.) was added at the ratio of two moles of phalloidin per mole of actin protomers. *In vitro* motility assay for the Cy3-gelsolin-actin sliding on HMM was done according to Toyoshima *et al.* (1987), except that the actin filaments were not stained with rhodamine phalloidin.

Actin filaments labelled with Cy3-maleimide

Fifty-six μmole of monofunctional Cy3-maleimide (Amersham Life Science, U.S.A.) was mixed with 20 μM of F-actin in F-buffer (10 mM MOPS, 0·1 M KCl, 1 mM MgCl$_2$, 0·3 mM NaN$_3$, pH 7·0) and incubated for 4 h at 0 °C. The reaction was terminated by the addition of 1·13 mM dithiothreitol, and the mixture was centrifuged at 346 000 g for 1 h. The pellet was homogenized, dialysed against G-buffer (5 mM Tris-HCl, 0·2 mM CaCl$_2$, 0·1 mM NaN$_3$, 0·2 mM ATP, pH 8·0), and centrifuged at 346 000 g for 1 h. The supernatant was polymerized in F-buffer. After several cycles of polymerization/depolymerization, unreacted Cy3-maleimide was separated from labelled G-actin on a Sephadex G-25 column (PD-10; Pharmacia, Sweden). About 30% actin was labelled, as estimated from $\epsilon_{\approx550\,nm} = 150\,000$ M^{-1} cm^{-1} for Cy3 (Ernst *et al.*, 1989) and $E^{1\%}_{290\,nm} = 6·3$ for G-actin (Houk & Ue, 1974). The labelled actin was mixed with unlabelled actin at various ratios and polymerized in F-buffer in the presence of twofold molar excess of phalloidin for 24 h at 0 °C. The ratios of Cy3-actin to unlabelled actin in the

polymerized samples were 1:4, 1:50, 1:250, 1:1200, 1:2500 after correction for the 30% labelling of the labelled actin sample. Motility assay for the Cy3-labelled actin sliding on HMM was done as in Sase *et al.* (1995), on a coverslip coated with polylysine (Ohichi *et al.*, 1993).

HMM labelled with Cy3-maleimide

HMM was dialysed against a solution containing 30 mM KCl, 25 mM Tris-HCl (pH 8·0) at 4 °C. HMM (1 mg mL^{-1}) was mixed with Cy3-maleimide (5·72 μM) and the mixture was incubated for 1 h at room temperature. The reaction was terminated with 300 μM dithiothreitol. The solution was centrifuged at 346 000 g for 1 h, and the supernatant was applied to a Sephadex G-25 column (PD-10; Pharmacia, Sweden) to remove unreacted Cy3.

Results

Using the conventional microscope (IX70) equipped with a standard mercury lamp and the SIT camera, we examined samples in which one of the dye-labelled proteins above was sufficiently diluted. We saw light spots on the monitor screen, as expected for single fluorophores distributed on a coverslip. Dotted appearance alone, however, does not mean that each spot really represented a single fluorophore. On a cleaned coverslip, we often found a small number of tiny light spots, of which some had intensities similar to those for the dye-labelled proteins. Presumably, these are dust particles, because the number tended to increase when cleaned coverslips were exposed to the air for a longer time. Some dust particles, even bright ones, were apparently photobleached in one step, in part due probably to their detachment and in part due to real photobleaching, although such a one-step behaviour is usually ascribed to single fluorophores. To distinguish between light emission from genuine single fluorophores and emission from dust or impurities, we designed three independent experiments in which the fluorophores were allowed to slide at a known velocity and/or quantitative measurements of spot intensities were carried out.

In the first experiment, single fluorophores (Cy3) were attached to the barbed ends of actin filaments, and the filaments were observed to slide on a coverslip coated with HMM in the presence of ATP. A steadily moving light spot would thus represent a Cy3 molecule, while spots corresponding to impurities, whether on the glass surface or bound to HMM, should remain stationary. Impurities in solution would undergo erratic Brownian motion, which, for nanometre-sized particles, is fast enough to blur and wipe out the spot image.

To ensure the presence of at most one fluorophore per moving actin filament, we exploited the property of gelsolin that this protein binds to the barbed (tail) end of an actin

filament at 1:1 ratio, as well as the property that only one Gln residue within gelsolin is targeted by transglutaminase (Katsura *et al.*, 1994). The latter property was confirmed as seen in the time-course of dansyl-cadaverine incorporation into gelsolin (Fig. 1). The amount of Cy3-cadaverine incorporated in gelsolin was also measured at one time point (the open circle in Fig. 1), showing a stoichiometry of slightly less than 1.

The labelled actin filaments were subjected to the conventional motility assay where coverslips were coated with nitrocellulose. The nitrocellulose film emitted very bright fluorescence, but it diminished completely within a few minutes due to photobleaching. Then, a number of small fluorescent spots were seen to move into the photobleached area from the periphery. Their velocity was $3{\cdot}8 \pm 0{\cdot}4\,\mu\mathrm{m\,s}^{-1}$ on average, while the sliding velocity of actin filaments fully labelled with rhodamine-phalloidin was $3{\cdot}7 \pm 0{\cdot}4\,\mu\mathrm{m\,s}^{-1}$ under the same conditions. Thus, the moving spots we observed with the conventional microscope were single Cy3 molecules, each attached to the barbed end of an actin filament.

In the second experiment, we attempted a quantitative
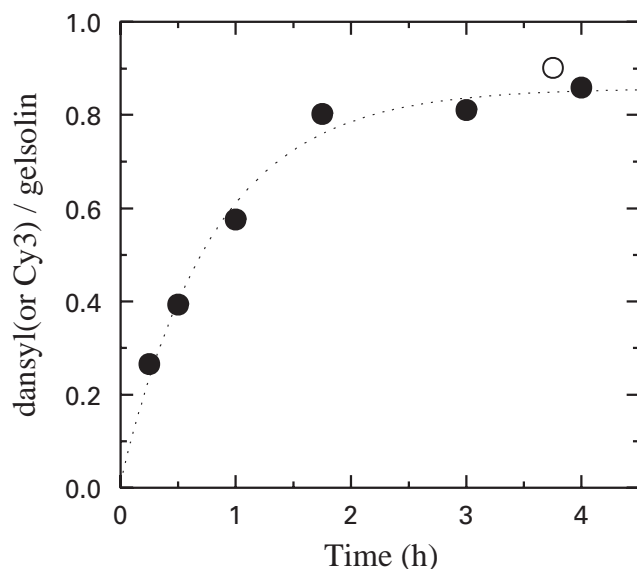
Fig. 1. Transglutaminase-catalysed incorporation of dansyl-cadaverine and Cy3-cadaverine into gelsolin. Closed circles, dansyl-cadaverine; open circle, Cy3-cadaverine. The amount of the dansyl fluorophore incorporated was estimated from the fluorescence intensity at 550 nm (with excitation at 330 nm) of labelled gelsolin that had been digested exhaustively with papain. Although the spectrum of dansyl fluorescence blue-shifted (from 550 nm to 522 nm) upon incorporation into gelsolin, digestion with papain completely reversed the spectral shift, justifying the fluorometric quantification. The amount of Cy3 incorporated into gelsolin was estimated from the absorbance at 552 nm of labelled gelsolin. Both types of amine-containing substrates gave similar near-saturation levels of incorporation (about 0·9).

measurement of fluorescence intensities. We labelled a reactive thiol (Cys374) of actin with Cy3-maleimide and made a series of filament preparations containing different proportions of labelled actin (Sase *et al.*, 1995). We observed the actin filaments bound to coverslips coated with polylysine (Fig. 2A–E). As the number of dye molecules in an actin filament decreased, the filament image changed from a uniform string to a collection of dots. At high labelling ratios where a filament was unambiguously recognized (Fig. 2C–E), the fluorescence intensity corresponding to a single fluorophore was estimated as the integrated intensity of the filament divided by the number of fluorophores per filament [(the filament length) × (366 actin protomers/μm filament) × (labelling ratio)]. At low labelling ratios (Fig. 2A–B), the integrated intensity of each spot was taken as the fluorescence intensity of a single fluorophore. As shown in Fig. 2(F), the fluorescence intensities estimated at various labelling ratios agreed with one another, indicating that most of the fluorescent spots at the lowest labelling ratios represented individual Cy3 fluorophores. To demonstrate that the spots represented genuine Cy3 fluorophores and not impurities, the actin filaments at the labelling ratio of 1:2500 were observed to slide over HMM bound to a coverslip coated with polylysine. Most spots with an intensity of a single fluorophore moved about on the coverslip (Fig. 3) at a velocity of about $1{\cdot}7\,\mu\mathrm{m\,s}^{-1}$, the sliding velocity expected on a polylysine surface (Sase *et al.*, 1997).

In the third experiment, we prepared HMM labelled with Cy3-maleimide at the reactive thiol SH1 (Funatsu *et al.*, 1995). When the labelled protein was examined on an uncoated coverslip, spots with basically two different intensities were observed (Fig. 4A). Correspondingly, the intensity distribution (Fig. 4B) showed two peaks, one at twice the intensity of the other. Fluorescent spots with an intensity around the second peak in Fig. 4(B) were photobleached in two steps with equal sizes (Fig. 4C). Because an HMM molecule has one each of SH1 in the two heads, the first and second peaks in Fig. 4(B) should correspond to single and two fluorophores, respectively. The mean time for photobleaching of one fluorophore was about 14 s.

The coefficient, α, that converts N_{AD} value to the number of photons/sec was estimated to be 7·3. The sum of N_{AD} values over 9×9 pixels, which enclosed a fluorescence spot of a Cy3-actin protomer, was 365 after subtraction of the background (Fig. 2F). The number of photons collected is therefore 2665. The total number of photons/s emitted by a Cy3-actin was calculated to be $3{\cdot}8 \times 10^4$. Thus, the collection efficiency is 7%. The N_{AD} value of the background was 42·6 (Fig. 4B), corresponding to 311 photons/s. For a single molecule of HMM labelled with one Cy3 the N_{AD} value, at a pixel giving the peak intensity, was 64·7 after subtracting the background (Fig. 4B). The signal-to-background ratio is therefore about 1·5.
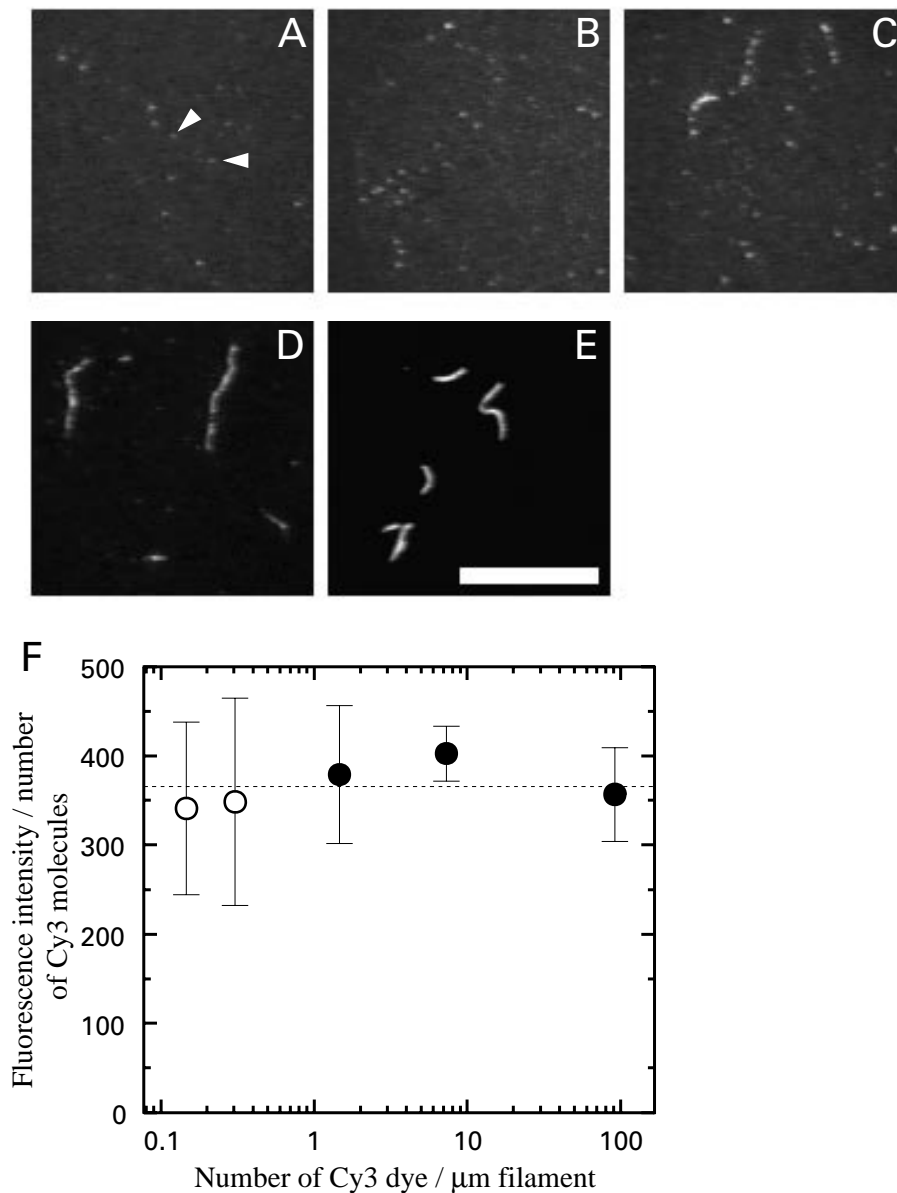
Fig. 2. (A–E) Fluorescence images of actin filaments at various Cy3 contents. The ratio of Cy3-labelled actin to unlabelled actin was 1:2500 (A), 1:1200 (B), 1:250 (C), 1:50 (D), and 1:4 (E). Scale bar, 20 μm (0·34 μm per pixel). All images were integrated over 16 video frames (0·53 s). The oblong appearance of the spot images (also in Figs 3 and 4) is a characteristic of the SIT camera used. The total intensity of the excitation light that emerged from the objective lens was 3·2 mW for images A, B and C, 0·8 mW for D, and 0·1 mW for E. (F) Fluorescence intensities (arbitrary units) for a single Cy3 molecule estimated from images as in A–E. The fluorescence intensities were corrected for the different excitation intensities. Although the images were integrated over 16 video frames, the intensities given here were those per video frame. Spot intensities in samples A and B (open circles) were obtained by integrating the intensity over a square enclosing the spot and subtracting a background integrated over an identical square near the spot. 40 spots were analysed for each sample, and the average and standard deviation are shown in the figure. Single Cy3 intensity in a filament image in samples C–E (closed circles) was estimated as follows: the filament was enclosed in a rectangle and the integrated intensity over the entire rectangle was calculated. A background intensity, estimated in an identical rectangle in a nearby filament-free area, was subtracted from the filament intensity. Then the intensity was divided by the number of Cy3 molecules expected on the actin filament. About 15 filaments were analysed for each sample.

Fig. 3. Movement of single Cy3 molecules carried by a sliding actin filament. Arrowheads show a spot with an intensity expected for a single Cy3 fluorophore moving from lower-right to upper-left. Double arrowheads show a spot twice as bright, presumably two Cy3 fluorophores closely apposed on a filament. Scale bar, $10 \, \mu$m. All images were integrated over 16 video frames. In the final image, the single-fluorophore spot disappeared due to photobleaching.

Fig. 4. (A) Fluorescence image of individual HMM molecules labelled with Cy3. Scale bar, $10 \, \mu$m ($0.34 \, \mu$m per pixel). The image was integrated over 16 video frames. Single and double arrowheads indicate HMM molecules with presumably one and two Cy3 molecules, respectively. (B) Distribution of spot intensities for Cy3-labelled HMM. The intensity here is the peak intensity of the light spot at the magnification of $0.34 \, \mu$m per pixel (each spot measures $\approx 4 \times 2$ pixels at half the peak intensity). Although the image was integrated over 16 video frames, the intensity is that per video frame. The value 255 on the horizontal axis indicates the saturation level of the SIT camera set at the maximal sensitivity. The dotted line indicates the camera dark level, and the dashed line the background level (the intensity of spot-free area). The two major peaks in the distribution are at 64.7 and 122.2 from the background level on the horizontal scale. (C) Quantised photobleaching of a fluorescent spot corresponding to two fluorophores. The ordinate is the peak intensity in the fluorescent spot, in the same scale as in B. The average lifetime with one fluorophore was 14 s.
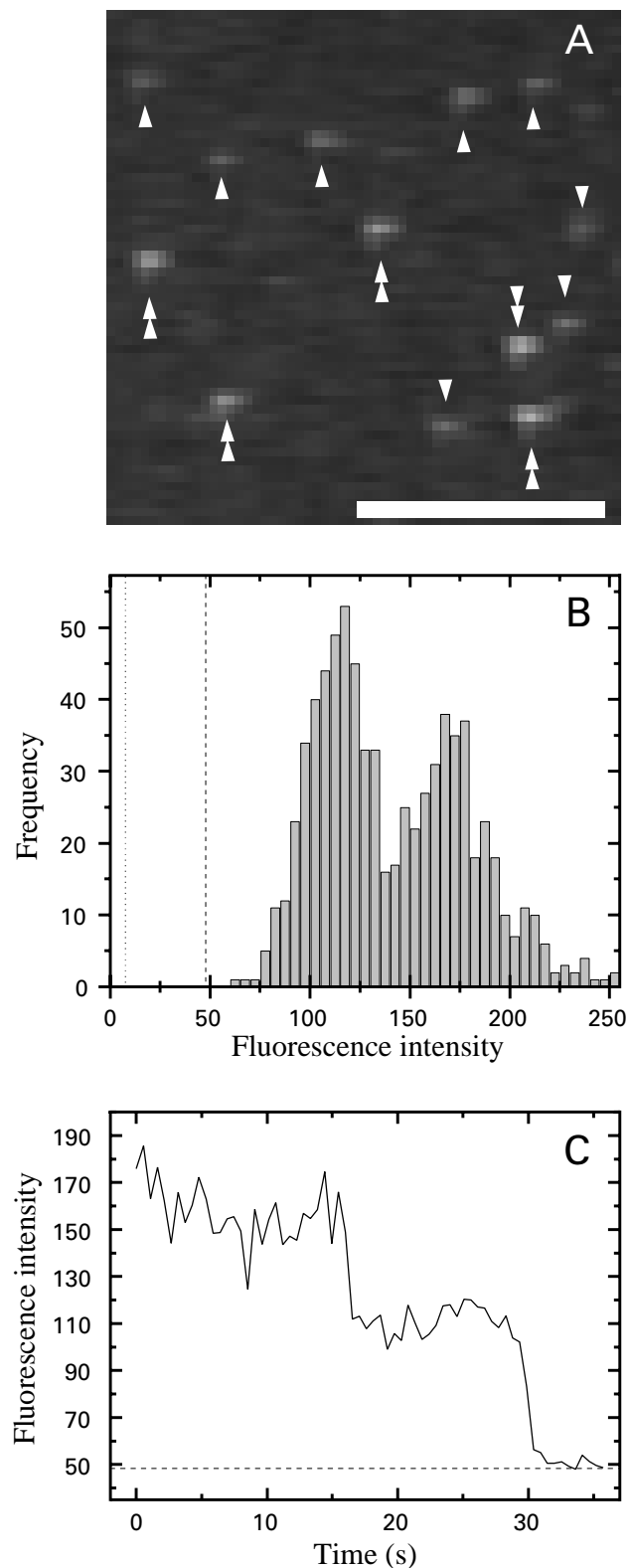
Discussion

We have shown that a commercial microscope allows one to visualize single fluorophores in an aqueous environment. The most encouraging finding is that the background is already low (the dashed line in Fig. 4B) without modification of the microscope and even with the oil-immersion objective. Expertise is no longer required for single-fluorophore imaging, although care has to be always exercised to avoid contamination with dust in the samples. The background intensity was quantified to be about 311 photons/s/pixel. This low background results from low reflection of light at the inner surfaces of the microscope and low reversion of the reflected light to the optical pass. The former is achieved by selecting a new black paint for coating the inner surfaces. The latter is achieved by minimizing the area of inner surfaces parallel to the optical path and by new design of the lens system (I. Endoh, personal communication).

Without any modification of a commercial microscope, we obtained the signal-to-background ratio of 1·5 for detection of a single Cy3 molecule attached to HMM. Here, we compare this value with the results obtained by the other methods, although the comparison cannot be accurate because the ratio largely depends on the size of a field stop used, which is not usually specified in literature. By extensively modifying a commercial microscope (different from ours) and replacing a standard high-pressure mercury lamp with a laser as excitation source, the signal-to-background ratio of 2·9–3·5 has been achieved for a single Cy3 molecule attached to HMM (Funatsu et al., 1995; Tokunaga et al., 1997) and for a single tetramethylrhodamine (TMR) molecule attached to actin (Sase et al., 1995). Total reflection microscopy, which confines the excitation light to a depth of about 150 nm from the coverslip–medium interface, can achieve the signal-to-background ratio of 160 in the prism-type (Funatsu et al., 1995) or 12 in the objective-type (Tokunaga et al., 1997) for detection of a single Cy3 molecule attached to HMM.

For single fluorophore detection the choice of fluorophore is also an important factor. It should be photoresistive and should have a high molar extinction coefficient as well as a high quantum yield. TMR that has often been used also possesses these attributes. We could detect single molecules of this fluorophore with the same setup as used for Cy3. Water-soluble fluorescent semiconductor nanocrystals must be another choice. It has recently been demonstrated that in all the attributes above they are superior to organic fluorophores (Bruchez et al., 1998; Chan & Nie, 1998), although further development seems required for them to be feasibly and widely used for biochemical applications.

In the present study fluorophores attached to proteins are always close to the surface of a coverslip. Because of this situation and the low background of the microscope, we did not have to confine the excitation light to the vicinity of the surface. In studies where fluorophores are present in the bulk solution as well as on the surface, it would be difficult to detect single fluorophores on the surface because of the large background signals from fluorophores in the bulk solution. In such studies total internal reflection is necessary for the selective excitation. Even in this case a microscope with the low background is quite helpful, because we do not have to modify the microscope itself.

Acknowledgements

References

Ando, T. (1984) Fluorescence of fluorescein attached to myosin SH1 distinguishes the rigor state from the actin-myosin-nucleotide state. *Biochemistry*, **23**, 375–381.

Ando, T. & Scales, D. (1985) Skeletal muscle myosin subfragment-1 induces bundle formation by actin filaments. *J. Biol. Chem.* **260**, 2321–2327.

Betzig, E. & Chichester, R.J. (1993) Single molecules observed by near-field scanning optical microscopy. *Science*, **262**, 1422–1425.

Bruchez, M. Jr, Moronne, M., Gin, P., Weiss, S. & Alivisatos, A.P. (1998) Semiconductor nanocrystals as fluorescent biological labels. *Science*, **281**, 2013–2016.

Chan, W.C.W. & Nie, S. (1998) Quantum dot bioconjugates for ultrasensitive nonisotopic detection. *Science*, **281**, 2016–2018.

Connellan, J.M., Chung, S.I., Whetzel, N.K., Bradley, L.M. & Folk, J.E. (1971) Structural properties of guinea pig liver transglutaminase. *J. Biol. Chem.* **246**, 1093–1098.

Craig, R. & Megerman, J. (1977) Assembly of smooth muscle myosin into side-polar filaments. *J. Cell Biol.* **75**, 990–996.

Dickson, R.M., Cubitt, A.B., Tsien, R.Y. & Moerner, W.E. (1997) On/off blinking and switching behaviour of single molecules of green fluorescent protein. *Nature*, **388**, 355–358.

Ernst, L.A., Gupta, R.K., Mujumdar, R.B. & Waggoner, A.S. (1989) Cyanine dye labeling reagents for sulfhydryl groups. *Cytometry*, **10**, 3–10.

Funatsu, T., Harada, Y., Tokunaga, M., Saito, K. & Yanagida, T. (1995) Imaging of single fluorescent molecules and individual ATP turnovers by single myosin molecules in aqueous solution. *Nature*, **374**, 555–559.

de Gennes, P.G. (1997) Molecular individualism. *Science*, **276**, 1999.

Harada, Y., Funatsu, T., Tokunaga, M., Saito, K., Higuchi, H., Ishii, Y. & Yanagida, T. (1998) Single molecule imaging and

nanomanipulation of biomolecules. *Methods Cell Biol.* **55**, 117–128.

Houk, T.W. Jr & Ue, K. (1974) The measurement of actin concentration in solution: a comparison of methods. *Anal. Biochem.* **62**, 66–74.

Ishijima, A., Kojima, H., Funatsu, T., Tokunaga, M., Higuchi, H., Tanaka, H. & Yanagida, T. (1998) Simultaneous observation of individual ATPase and mechanical events by a single myosin molecule during interaction with actin. *Cell*, **92**, 161–171.

Katsura, H., Doi, Y., Janado, M., Ooi, T. & Motoki, M. (1994) A study on the structure of the actin-gelsolin complex. *Biophys.* **34** (Suppl. s118), (in Japanese).

Kinosita, K. Jr, Yasuda, R., Sase, I. & Miyata, H. (1997) Attempts to visualize conformational changes in a single protein molecule during function. *Microsc. Microanal.* **3**, (Suppl. 2), 799–800.

Kunioka, Y. & Ando, T. (1996) Innocuous labeling of the subfragment-2 region of skeletal muscle heavy meromyosin with a fluorescent polyacrylamide nanobead and visualization of individual heavy meromyosin molecules. *J. Biochem.* **119**, 1024–1032.

Kurokawa, H., Fujii, W., Ohmi, K., Sakurai, T. & Nonomura, Y. (1990) Simple and rapid purification of brevin. *Biochem. Biophys. Res. Commun.* **168**, 451–457.

Lowry, O.H., Rosebrough, N.J., Farr, A.L. & Randall, R.J. (1951) Protein measurement with the folin phenol reagent. *J. Biol. Chem.* **193**, 265–275.

Lu, H.P. & Xie, X.S. (1997) Single-molecule spectral fluctuations at room temperature. *Nature*, **385**, 143–146.

Moerner, W.E. & Kador, L. (1989) Optical detection and spectroscopy of single molecules in a solid. *Phys. Rev. Lett.* **62**, 2535–2538.

Nishizaka, T., Miyata, H., Yoshikawa, H., Ishiwata, S. & Kinosita, K. Jr (1995) Unbinding force of a single motor molecule of muscle measured using optical tweezers. *Nature*, **377**, 251–254.

Ohichi, T., Hozumi, T. & Higashi-Fujime, S. (1993) *In vitro* motility of proteolytically cleaved myosin subfragment 1 on a lysine-coated surface. *J. Biochem.* **114**, 299–302.

Perkins, T.T., Smith, D.E. & Chu, S. (1997) Single polymer dynamics in an elongational flow. *Science*, **276**, 2016–2021.

Sase, I., Miyata, H., Corrie, J.E.T., Craik, J.S. & Kinosita, K. Jr (1995) Real time imaging of single fluorophores on moving actin with an epifluorescence microscope. *Biophys. J.* **69**, 323–328.

Sase, I., Miyata, H., Ishiwata, S. & Kinosita, K. Jr (1997) Axial rotation of sliding actin filaments revealed by single-fluorophore imaging. *Proc. Natl. Acad. Sci. USA*, **94**, 5646–5650.

Spudich, J.A. & Watt, S. (1971) The regulation of rabbit skeletal muscle contraction. I. Biochemical studies of the tropomyosin-troponin complex with actin and the proteolytic fragments of myosin. *J. Biol. Chem.* **246**, 4866–4871.

Suzuki, N., Miyata, H., Ishiwata, S. & Kinosita, K. Jr (1996) Preparation of bead-tailed actin filaments: estimation of the torque produced by the sliding force in an *in vitro* motility assay. *Biophys. J.* **70**, 401–408.

Tokunaga, M., Kitamura, K., Saito, K., Iwane, A.H. & Yanagida, T. (1997) Single molecule imaging of fluorophores and enzymatic reactions achieved by objective-type total internal reflection fluorescence microscopy. *Biochem. Biophys. Res. Commun.* **235**, 47–53.

Toyoshima, Y.Y., Kron, S.J., McNally, E.M., Niebling, K.R., Toyoshima, C. & Spudich, J.A. (1987) Myosin subfragment-1 is sufficient to move actin filaments *in vitro*. *Nature*, **328**, 536–539.

Vale, R.D., Funatsu, T., Pierce, D.W., Romberg, L., Harada, Y. & Yanagida, T. (1996) Direct observation of single kinesin molecules moving along microtubules. *Nature*, **380**, 451–453.

Weeds, A.G. & Pope, B. (1977) Studies on the chymotryptic digestion of myosin. Effect of divalent cations on proteolytic susceptibility. *J. Mol. Biol.* **111**, 129–157.